Luminescence properties of the Cu4I62− cluster

ARTICLE *in* CRYSTENGCOMM · JUNE 2011

Impact Factor: 4.03 · DOI: 10.1039/C0CE00909A

6 AUTHORS, INCLUDING:

Rong-Zhen Liao
Stockholm University
50 PUBLICATIONS **545** CITATIONS
SEE PROFILE

Hjalmar Brismar
KTH Royal Institute of Technology
133 PUBLICATIONS **4,126** CITATIONS
SEE PROFILE

Fredrik Laurell
KTH Royal Institute of Technology
381 PUBLICATIONS **3,916** CITATIONS
SEE PROFILE

Sven Lidin
Lund University
287 PUBLICATIONS **2,773** CITATIONS
SEE PROFILE

CrystEngComm

Dynamic Article Links

Cite this: *CrystEngComm*, 2011, **13**, 4729

www.rsc.org/crystengcomm

PAPER

Luminescence properties of the $Cu_4I_6^{2-}$ cluster†

Ehsan Jalilian,*[a] Rong-Zhen Liao,[b] Fahmi Himo,[b] Hjalmar Brismar,[c] Fredrik Laurell[d] and Sven Lidin[e]

Received 3rd December 2010, Accepted 18th March 2011
DOI: 10.1039/c0ce00909a

Two new solvates were prepared in the system Cu(I)I using a solvolysis reaction. The structures for both of them were solved by X-ray crystallography, showing that they constitute two modifications of the same compound with the net formula $[Cu_4I_6](P(C_6H_5)_4)_2 \cdot 2OC(CH_3)_2$. Both types of crystals show vivid fluorescence when exposed to UV light. The formation of the first modification (I) seems to be preferred by kinetics and on ageing in the mother liquor it converts to modification (II). The Cu positions in (I) are disordered while those in (II) are fully ordered. The luminescent properties of both crystals were characterized using a confocal microscope and an excitation wavelength of 405 nm, resulting in fluorescence spectra with the intensities of 1.22 and 0.52 relative to the reference (fluorescein 10 μM). Density functional theory calculations on the ordered $Cu_4I_6^{2-}$ core of modification (II) show that the de-excitation from LUMO to HOMO is responsible for the luminescence. The calculated emission spectrum has a maximum at 531 nm in good agreement with the results from confocal microscopy.

Introduction

Iodocuprates(I) exhibit a very interesting structural chemistry because of their wide variation in local Cu–I coordination. Consequently, a large number of distinct cluster compounds are known ranging from the simple mononuclear ions such as $[CuI_2]^-$ and $[CuI_3]^{-2}$, the binuclear ions $[Cu_2I_4]^{-2}$ and $[Cu_2I_6]^{-4}$ and the tetranuclear species $[Cu_4I_6]^{-4}$ and $[Cu_4I_4R_4]^0$ where R is a donor such as an amine, a phosphine or a thiol to very complex species such as $[Cu_5I_7]^{-2}$, $[Cu_8I_{13}]^{-5}$ and $[Cu_{36}I_{56}]^{-20}$ and polymers such as $[CuI_2]^-{}_\infty$, $[Cu_2I_3]^-{}_\infty$, $[Cu_3I_4]^-{}_\infty$ and $[Cu_4I_6]^{-2}{}_\infty$.[1,2] Perhaps the most remarkable halocuprate polyanion is the $[Cu_3I_4]^-{}_\infty$, infinite chain in $[(C_6H_5)_4P][Cu_3I_4]$, a Boerdijk–Coxeter helix (BC helix) with a small perturbation that makes it periodic, the same arrangement repeating after the eight full turns, forming a chiral helix.[3]

The diversity in Cu(I) geometry and the bridging capability of iodide yield this unique flexibility. The Cu–Cu distance may be quite short, frequently below 2.7 Å, and even approaching the Cu–Cu distance in the element (2.56 Å). A very interesting feature is the strong fluorescence in the electro-neutral, hetero-cubane type $[Cu_4X_4R_4]^0$ (X = Cl, Br or I) species that has been extensively studied.[4–6] Less has been written about the luminescence properties of the other cluster species, and in particular about the much rarer species $[Cu_4I_6]^{-2}$. This is natural, given that this cluster has been reported in ten instances and the Cu positions display disorder in nine of them.[7–12] In the tenth compound,[13] the cluster coexists with a $[Cu_8I_{13}]^{-5}$ cluster, making it difficult to study the fluorescent properties of $[Cu_4I_6]^{-2}$ in isolation. Further, in this compound the positions of the counter-ions are not reported, signaling disorder on the cationic sub-structure. Hence, this paper constitutes the first report of a compound featuring a fully ordered of $[Cu_4I_6]^{-2}$ cluster. The Cu_4I_6 cluster is quite regular with Cu–Cu distances in the range 2.69–2.88 Å and Cu–I distances in the range 2.56–2.58 Å for both compounds. These values are similar to those given in the earlier reports,[7–13] where these values range from 2.36–2.82 Å for Cu–I and 2.67–3.13 Å for Cu–Cu. In particular for the compound "potassium hexakis(12-crown-4-potassium) hexakis(μ_2-iodo)-tetra-copper(I) (μ_8-iodo)-dodecakis(μ_2-iodo)-octa-copper(I) monohydrate" where the $[Cu_4I_6]^{-2}$ cluster is ordered these distances are Cu–Cu 2.71–2.81 Å and Cu–I 2.55–2.99 Å. Whether the differences are due to the disorder in previously reported compounds or a sign of a general flexibility in the Cu_4I_6 cluster is an open question. A critical parameter in the Cu–I system is believed to be the relatively short Cu–Cu distances (d [Cu–Cu] < 2.8 Å). In complexes that have longer Cu–Cu distances the luminescence is less pronounced.[4]

Aim

The system Cu–I–$P(C_6H_5)_4^+$ in acetone has been studied extensively, and contains a number of interesting compounds. Apart

[a]*Dept. of Material and Environmental Chemistry, Arrhenius Laboratory, Stockholm University, SE-106 91 Stockholm, Sweden. E-mail: ehsan.jalilian@mmk.su.se; Fax: +46 8 152 147; Tel: +46 8 161 258*
[b]*Dept. of Organic Chemistry, Arrhenius Laboratory, Stockholm University, SE-106 91 Stockholm, Sweden. E-mail: himo@organ.su.se; Fax: +46 8 154 908; Tel: +46 8 161094*
[c]*Royal Inst. Technol, KTH, Albanova, Univ. Ctr, Dept. Cell Phys, SE-106 91 Stockholm, Sweden. E-mail: hjalmar@cellphysics.kth.se; Fax: +46 8 553 782 16; Tel: +46 8 161 015*
[d]*Royal Inst. Technol, KTH, SE-106 91 Stockholm, Sweden. E-mail: fl@laserphysics.kth.se; Fax: +46 8 553 782 16; Tel: +46 8 553 78153*
[e]*Dept. of Polymer and Material Chemistry, Lund University, SE-221 00 Lund, Sweden. E-mail: sven.lidin@polymat.lth.se; Fax: +46 222 4769; Tel: +46 222 4012*

† CCDC reference numbers 814686 and 814687. For crystallographic data in CIF or other electronic format see DOI: 10.1039/c0ce00909a

from $[(C_6H_5)_4P][Cu_3I_4]$ with the helical structure mentioned previously, Hartl *et al.*[14] report the discovery of two forms of $[(C_6H_5)_4P]_2[Cu_2I_4]$, and an additional two forms are reported by Pfitzner and Schmitz.[15] Nothing has been reported on the luminescence of these compounds, and this study was launched in order to assess this, and if possible, to study the stabilization of the various compounds that form in this system.

Methods

Synthesis

Cu powder, iodine and tetraphenylphosphonium were mixed and heated in different solvents under nitrogen atmosphere. When the solution became pale yellow it was hot-filtered,[3] the filtrate was cooled and left for several days at −10 °C while the solvent was allowed to evaporate slowly. From the acetone solution, three different types of crystals were observed, yellow (I), green (II) and colorless (III); from cyclopropyl methyl ketone or hydroxyacetone the BC helix structure of $[(C_6H_5)_4P][Cu_3I_4]$ is produced while from 4-methyl-2pentanon and 2-hexanon a monoclinic structure with composition $[P(C_6H_5)_2][Cu_2I_4]$ is produced. This compound is known from the work of Hartl *et al.*[14] The yield of the synthesis was well reproducible from one synthetic batch to the next, if the synthesis was given sufficient time to go to completion. Because of the several transient compounds formed and transformed during the course of the synthesis, it is only meaningful to calculate the yield of the final product stable under the mother liquor. The yield of this compound is approximately 5% based on the limiting reactant, iodide.

Single crystal diffraction

Diffraction data from the crystals were collected at $T = 100$ K on an Xcalibur3 single crystal diffractometer from Oxford diffraction. The data evaluation and absorption correction were carried out using CrysAlis[16] software package.

The structures for the crystals (I) and (II) were solved using charge flipping[17] as implemented in the program Superflip.[18] Jana2000[19] was used for refinement of the structures. Superflip readily produced the positions for I, Cu, P and a major part of the C atoms. For the determination of the remaining C and O positions difference Fourier analysis was used. The positions of two H atoms in acetone were also determined by difference Fourier analysis. These H atoms were then restrained to have a distance of 1.00 Å and an angle of 109.47° with the C backbone. The rest of the H atoms were located by geometrical methods.

Luminescence

To quantify the emission spectra a confocal microscope (Zeiss LSM510 META) was used and the local luminescence intensity was recorded and compared to a luminescence reference standard of 10 μM fluorescein in dH_2O. For excitation a continuous wave UV laser at 405 nm was used.

The emission spectra were collected with a VARIAN fluorescent spectrophotometer at ambient temperature (298 K) and low temperature (92 K) for both crystals.

Computational details

The calculations were carried out for the ordered $Cu_4I_6^{2-}$ core of modification (II) using density functional theory with the hybrid B3LYP[20] functional as implemented in the Gaussian09 program package.[21] The small-core relativistic effective core potentials, ECP10MDF and ECP28MDF, were employed for Cu and I, respectively, with the corresponding correlation consistent valence basis set cc-pVDZ.[22–24] Ground state geometry optimization was performed under T_d symmetry constraints. Analytical frequency calculations were done to check if it is a true minimum (without imaginary frequencies). For the optical absorption spectrum, the 20 lowest spin allowed singlet–singlet transitions (T_d symmetry) were calculated using TDDFT. The first symmetry-allowed excited singlet state was optimized using the TDDFT method without symmetry constraints. The optimized structure was then used for emission spectrum calculations using TDDFT. To model the polarization effect of the crystal environment, the polarizable continuum model (PCM) method[25] was used in the TDDFT calculations on the gas phase optimized structure. Two representative dielectric constants were selected, 4 and 80. Isodensity surface plots were constructed using the GaussView 4 program.[21]

Results

The colorless crystals (III) are identical to a phase produced by Hartl *et al.* earlier.[14] They exhibit weak luminescence. The crystals of types (I) and (II) proved to be new phases. These both have the composition $[P(C_6H_5)_4]_2^+[Cu_4I_6]^{2-}\cdot 2OC(CH_3)_2$ but their crystal structures are quite distinct. The stacking of $[P(C_6H_5)_4]^+$ and $[Cu_4I_6]^{-2}$ units in the two compounds is different, and while the $[Cu_4I_6]^{-2}$ units in (II) are fully ordered, the same complex in (I) exhibits the Cu disorder reported for most of the previously reported instances of this cluster.[13] The asymmetric unit in compound (I) contains a tetraphenylphosphonium (TPP) cation in a general position and half of the anion, $[Cu_4I_6]$, about an inversion center. The occupancy of the copper atoms is 0.5. The asymmetric unit for compound (II) is quite similar, again a TPP cation in a general position while the half of the anion, $[Cu_4I_6]$, is lying about a 2-fold axis instead. In compounds (I) and (II) the solvent (acetone) enters the structure in a very similar configuration, one formula unit of acetone per $2[PC_{24}H_{20}][Cu_4I_6]$. The oxygen in the acetone is coordinating to three phenyl rings from two different tetraphenylphosphonium ions and forms a cage-like network that surrounds the Cu–I complex.

The type (I) crystals are quite unstable, and after a few weeks storage in the mother liquor at 0 °C they are converted into type (II) crystals.

They are also susceptible to amorphization in the absence of solvent when stored at room temperature, but they may be stored for weeks without apparent damage if separated from the mother liquor and kept at −10 °C. They crystallize in space group $P\bar{1}$ ($a = 11.0794(2)$ Å, $b = 11.1586(2)$ Å, $c = 11.8673(2)$ Å, $\alpha = 82.422(17)°$, $\beta = 88.3512(14)°$, $\gamma = 88.9145(14)°$, $V = 5796.15(6)$ Å^3), $Z = 2$ (Conf. Fig. 1).

The type (II) crystals appear to be much more stable than type (I), and they may be stored in the mother liquor. They crystallize

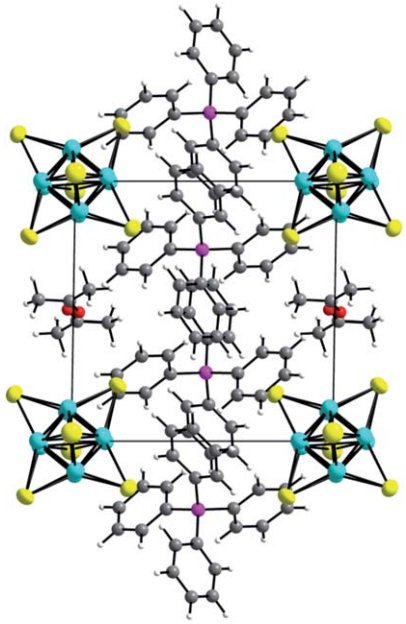

Fig. 1 Unit cell of the type (I) crystal, $P\bar{1}$ viewed along the *c* axis. The yellow ellipsoids represent the iodide atom while the blue represent the copper atoms, the purple spheres are for phosphorus, the grey are for carbon atoms and the white are the hydrogen atoms. This color scheme is followed throughout the paper.

in space group *Pbcn* ($a = 15.09870(8)$ Å, $b = 15.53354(7)$ Å, $c = 24.71324(18)$ Å, $V = 5796.15(6)$ Å^3), $Z = 4$ (Conf. Fig. 2).For crystallographic details about both structures see Table 5.

Both type (I) and type (II) crystals are strongly luminescent. Type (I) exhibits vivid yellow luminescence under UV light excitation while type (II) shows a more greenish luminescence. The type (III) crystal that contains a different CuI cluster is also luminescent, but only weakly so.

The luminescence spectrum for the type I and type II crystals can be seen in Fig. 3 and 5. The intensities were 1.22 respectively 0.52 relative to the standard fluorescein solution, which is a very strong emission.

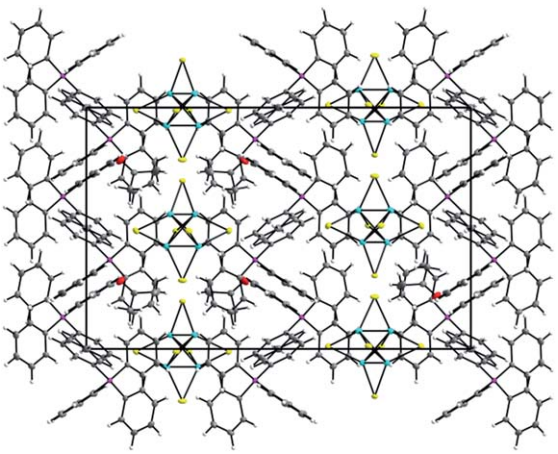

Fig. 2 Unit cell of type (II) crystal, *Pbcn*, viewed along the *a* axis.

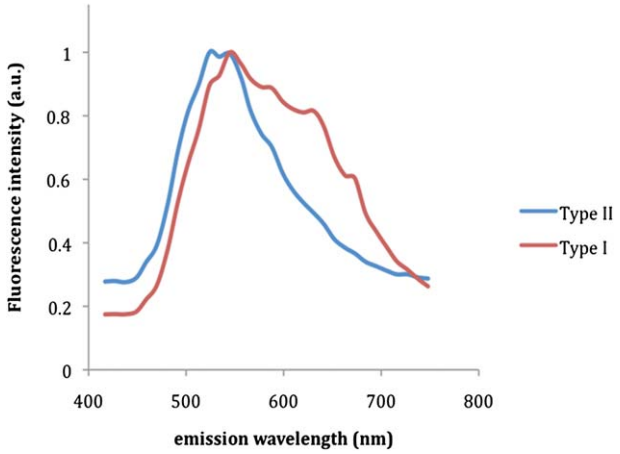

Fig. 3 Luminescence emission spectra of type I and II crystals excited at 405 nm.

Interestingly, the luminescence emission seems to be a surface effect as can be seen in Fig. 4, where a 3D stack of confocal images is rendered showing no emission from the interior of the crystal. This is possibly caused by reabsorption of emission from the interior of the crystal. The fact that luminescence was detectable also for crystals in the mother liquor indicates that it is a real property of the compounds under study, but to exclude the possibility that the luminescence was due to a thin surface layer of oxidation products on the surface of the crystals, a part of a sample was crushed under N_2 during illumination with ultraviolet light. The powder was brightly luminescent. To perform further studies on the powdered sample did however prove difficult due to the tendency of the compound to lose solvent. Luminescence spectroscopy shows that the lifetime of the luminescence is shorter than 0.1 ms for both compounds.

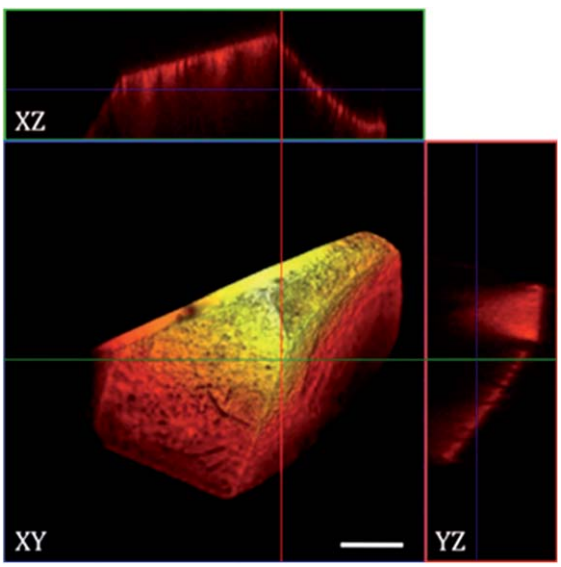

Fig. 4 3D rendering of a confocal stack of images with *XZ* and *YZ* projections of a type I crystal. The cross-section along the green line is shown in the top panel and the red line is shown to the right. Luminescence is only detected from the surface of the crystal. Scale bar is 100 μm.

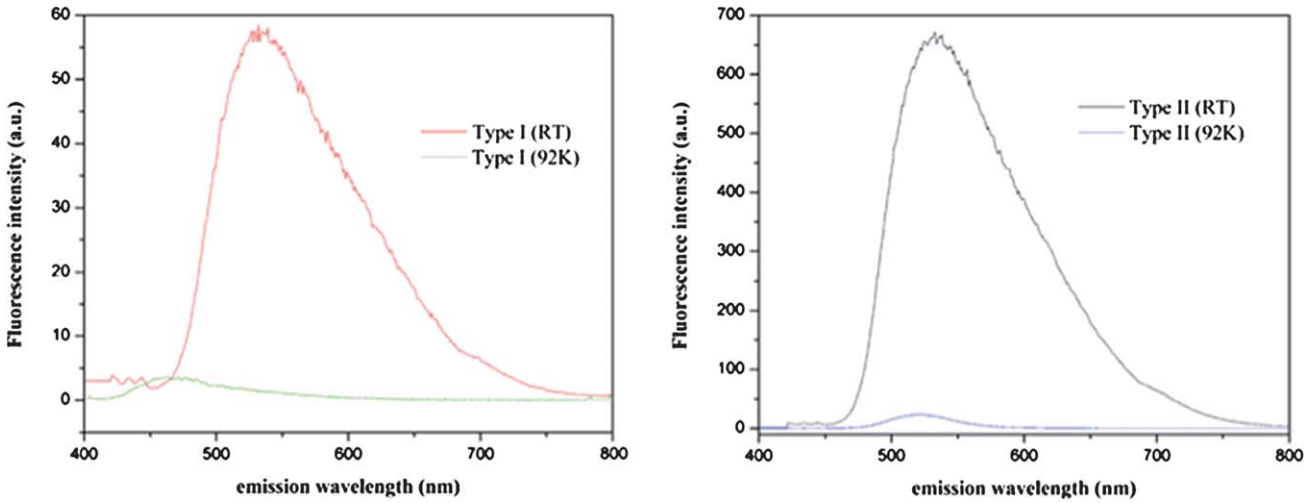

Fig. 5 Emission spectrum for both type, collected at ambient temperature (RT) and low temperature (92 K). The temperature dependency of the luminescence intensity and emission maximum is clearly shown.

Discussion and conclusions

Optimized geometry and electronic structure of the ground state

The optimized geometry of the ground singlet state is shown in Fig. 6. Some main geometric parameters are compared with the X-ray structure in Table 1. The geometric parameters from our calculations are in reasonably good agreement with X-ray data. The largest deviation is the Cu–I distance, which is overestimated by about 0.1 Å. Frequency calculations show that the complex in T_d symmetry has no imaginary frequency, evidencing that it is a true local minimum. Geometric relaxation from T_d to C_1 was negligible and the associated energy gain is only 0.1 kcal mol^{-1}. Isodensity surface plots of selected molecular orbitals (MOs) are reported in Fig. 7.

The 8 highest occupied MOs are combinations of copper d orbitals and iodine p orbitals. The HOMO orbitals are triple-degenerate and belong to T2 symmetry. These are followed by triple-degenerate orbitals with T1 symmetry and double-degenerate orbitals with E symmetry. The energies of these 8 orbitals are quite close, ranging from +0.20 to +0.42 eV.

The reason for the positive orbital energy is that the complex is doubly anionic. Both LUMO and LUMO + 1 belong to A1 symmetry. The LUMO has a bonding character of the cubic Cu_4 and an anti-bonding character of the Cu–I bonds, which is quite

Table 1 Optimized geometric parameters of $Cu_4I_6^{2-}$ in the S_0, S_1 states, with comparison to the X-ray structure data. (Distances in angstrom and angles in degrees.) S_0 was optimized under T_d symmetry while S_1 was optimized without symmetry constraints

Parameters	Expt	S_0	S_1
Cu–Cu	2.69–2.88	2.77	2.55–2.62
Cu–I	2.56–2.58	2.67	2.70–2.80
∠Cu–Cu–Cu	57.1–64.1	60.0	59.2–61.7
∠Cu–Cu–I[a]	55.6–58.6	58.8	60.5–64.2
∠Cu–I–Cu[a]	62.8–68.6	62.4	55.4–57.3

[a] I is the one bridging the two coppers.

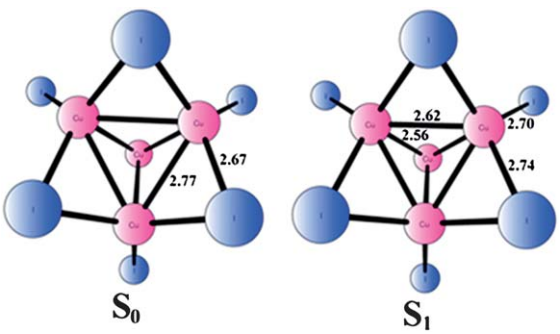

Fig. 6 Optimized structures of the S_0 (T_d) and S_1 (C_1) states of $Cu_4I_6^{2-}$. Distances in angstrom.

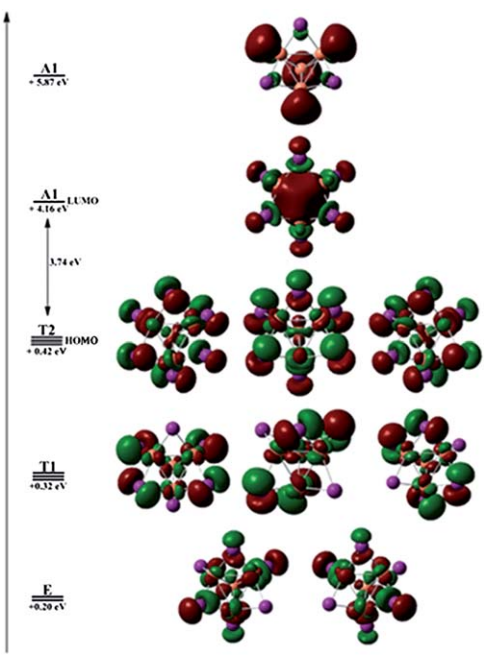

Fig. 7 Schematic representation and isodensity surface plots of selected molecular orbitals for the ground state.

Table 2 Composition of main orbital singlet–singlet transitions of $Cu_4I_6^{2-}$ (T_d symmetry) in gas phase

Excited state	Nature of main transition (coefficients greater than 0.15)
1	HOMO − 5 → LUMO (−0.627) HOMO − 4 → LUMO (0.277)
2	HOMO − 3 → LUMO (−0.673)
3	HOMO − 4 → LUMO (0.615)
4	HOMO − 2 → LUMO (0.633) HOMO → LUMO (−0.294)
5	HOMO − 2 → LUMO (0.294) HOMO → LUMO 0.634)
6	HOMO − 1 → LUMO (0.698)
7	HOMO − 7 → LUMO (0.671) HOMO − 6 → LUMO (0.176)
8	HOMO − 7 → LUMO (−0.176) HOMO − 6 → LUMO (0.671)

similar to observations made in previous theoretical studies on $[Cu_4I_4(pyridine)_4]$.[26–28] The HOMO–LUMO gap is calculated to be 3.74 eV. Since HOMO and LUMO belong to T2 and A1 symmetry, respectively, the HOMO–LUMO excitation will be symmetry-allowed, while T1 and E to A1 excitations will be symmetry-forbidden.

Optical absorption spectrum

The 20 lowest excited singlet states were obtained using TDDFT calculations. In all these excitations, the electron goes to LUMO, which belongs to A1 symmetry as discussed above. Therefore, only excitations from T2 symmetry orbitals are allowed. The lowest symmetry-allowed energy transition is calculated to be triple-degenerate at 444 nm in gas phase, which is slightly shifted to 440 nm and 437 nm, when using the solvation model with dielectric constants 4 and 80, respectively. The calculated absorption wavelength is in reasonable agreement with the experimental value of 405 nm, which is the lowest absorption. The transition oscillator strength increases from 0.0294 in gas phase to 0.0403 with eps = 80. Thus, the solvation effects do not lead to significant changes for the absorption spectrum for this complex. These three excitations (states 4, 5, and 6) are from HOMO, HOMO − 1, and HOMO − 2 to LUMO (see Table 2).

The next allowed transition is at 340 nm in gas phase, corresponding to HOMO − 15, HOMO − 14, and HOMO − 13 excitation to LUMO. Excited states 1, 2, and 3 belong to the T1 symmetry, corresponding to HOMO − 3, HOMO − 4, and HOMO − 5 excitation to LUMO. These are symmetry-forbidden, likewise higher excited states 7 and 8 are transitions from HOMO − 6 and HOMO − 7 to LUMO, which are of E symmetry.

We also calculated the absorption spectrum using the crystal structure geometry. Eight excited states are shown in Table 3.

The first three states have sizeable absorption intensity. From the nature of transitions, we can see that these three correspond to the T2 excited states 4, 5, and 6 under T_d symmetry. The lowest absorption wavelength is at 403 nm, which has some blue shift compared with the one under T_d symmetry. The higher excited states 4 to 8 have very weak intensity, which match the three T1 and two E excited states shown in Table 4. This is mainly due to the symmetry relaxation.

Singlet excited states: emission

Since luminescence is observed from the experiment, only emission from singlet excited state is considered in our calculations. From the ground state structure, we performed a TDDFT optimization of the first symmetry-allowed singlet excited state, which is characterized to be HOMO–LUMO excitation. During the geometry optimization, the symmetry is allowed to be lowered to C_1. The optimized S_1 structure is shown in Fig. 6, and is very close to C_{3v} symmetry. As discussed above, the LUMO contains cubic Cu_4 bonding and Cu–I anti-bonding character. Thus the excitation will induce contraction of the cubic copper cluster. In the optimized S_1 state, the Cu–Cu distances are shortened by 0.18 Å, to 2.59 Å in average, while the Cu–I

Table 3 Composition of main orbital singlet–singlet transitions of $Cu_4I_6^{2-}$ based on the crystal structure geometry

Excited state	Transition wavelength, λ/nm	Oscillator strength, f	Nature of main transition (coefficients greater than 0.15)
1	403.1	0.0249	HOMO − 2 → LUMO (−0.217) HOMO → LUMO (0.655)
2	401.9	0.0187	HOMO − 1 → LUMO (0.692)
3	400.7	0.0234	HOMO − 2 → LUMO (0.656) HOMO → LUMO (0.214)
4	396.7	0.0004	HOMO − 3 → LUMO (−0.673)
5	395.9	0.0004	HOMO − 4 → LUMO (0.682)
6	390.7	0.0001	HOMO − 5 → LUMO (0.680)
7	381.5	0.0001	HOMO − 6 → LUMO (0.684)
8	363.8	0.0002	HOMO − 7 → LUMO (0.687)

Table 4 Calculated TDDFT singlet–singlet excitation wavelengths and oscillator strengths of $Cu_4I_6^{2-}$ (T_d symmetry)

		Gas phase		eps = 4		eps = 80	
Excited state	Symmetry	Transition wavelength, λ/nm	Oscillator strength,f	Transition wavelength, λ/nm	Oscillator strength, f	Transition wavelength, λ/nm	Oscillator strength f
1, 2, 3	T1	446.2	0	441.5	0	438.8	0
4, 5, 6	T2	444.3	0.0294	440.4	0.0399	437.2	0.0403
7, 8	E	426.1	0	423.9	0	421.4	0
9, 10, 11	T1	387.7	0	383.1	0	380.0	0
12, 13, 14	T2	340.4	0.0370	339.0	0.0513	337.5	0.0507

Table 5 Crystallographic data

Compound reference	Crystal type (I)	Crystal type (II)
Chemical formula	$2(C_{24}H_{20}P)\cdot(Cu_4I_6)\cdot OC(CH_3)_2$	$C_{24}H_{20}P\cdot_0.5(Cu_4I_6)\cdot C_3H_6O$
Formula mass	1752.5	905.3
Crystal system	Triclinic	Orthorhombic
a/Å	11.0794(2)	15.1257(1)
b/Å	11.1586(2)	15.5606(1)
c/Å	11.8673(2)	24.7564(2)
α/°	82.4220(17)	90
β/°	88.3512(14)	90
γ/°	88.9145(14)	90
Unit cell volume/Å^3	1453.58(4)	5826.79(7)
Temperature/K	100	100
Space group	$P\bar{1}$	*Pbcn*
No. of formula units per unit cell, Z	1	8
Radiation type	Mo Kα	Mo Kα
Absorption coefficient, μ/mm^{-1}	4.717	4.712
No. of reflections measured	51 193	87 725
No. of independent reflections	8360	8685
R_{int}	0.0860	0.0177
Final R_1 values ($I > 2\sigma(I)$)	0.0414	0.0340
Final w$R(F^2)$ values ($I > 2\sigma(I)$)	0.0855	0.1075
Final R_1 values (all data)	0.1599	0.0379
Final w$R(F^2)$ values (all data)	0.1044	0.1092
Goodness of fit on F^2	1.24	1.80

distances are elongated by 0.07 Å, to 2.74 Å in average. At the S_1 geometry, the transition from the ground state to S_1 is calculated to be at 531 nm with $f = 0.0290$, which corresponds to the HOMO–LUMO excitation. Inclusion of solvation effects results in a blue shift of the emission and an increase of the intensity, which is the same as for the absorption. For example, when $\varepsilon = 80$ is used, the transition is at 520 nm with $f = 0.0400$. The calculated emission wavelength is thus in good agreement with the experimental observation, which has a broad peak around 500–700 nm (Fig. 3 and 5).

In conclusion, for $Cu_4I_6^{2-}$, three degenerate excitations, including the HOMO–LUMO transition, are symmetry-allowed and match the experimental absorption wavelength. The de-excitation from LUMO to HOMO accounts for the intensive luminescence.

References

1 U. Bentrup, M. Feist and E. Kemnitz, *Prog. Solid State Chem.*, 1999, **27**, 75–129.
2 J. H. Yu, H. B. Jia, L. Y. Pan, Q. X. Yang, T. G. Wang, J. Q. Xu, X. B. Cui, Y. J. Liu, Y. Z. Li, C. H. Lu and T. H. Ma, *J. Solid State Chem.*, 2003, **175**, 152–158.
3 H. Hartl and F. Mahdjourhassanabadi, *Angew. Chem., Int. Ed. Engl.*, 1994, **33**, 1841–1842.
4 P. C. Ford, E. Cariati and J. Bourassa, *Chem. Rev.*, 1999, **99**, 3625–3647.
5 M. H. Bi, G. H. Li, Y. C. Zou, Z. Shi and S. H. Feng, *Inorg. Chem.*, 2007, **46**, 604–606.
6 N. P. Rath, E. M. Holt and K. Tanimura, *Inorg. Chem.*, 1985, **24**, 3934–3938.
7 A. Nurtaeva and E. M. Holt, *Acta Crystallogr., Sect. C: Cryst. Struct. Commun.*, 1999, **55**, 1453–1457.
8 K. V. Domasevitch, J. A. Rusanova, O. Y. Vassilyeva, V. N. Kokozay, P. J. Squattrito, J. Sieler and P. R. Raithby, *J. Chem. Soc., Dalton Trans.*, 1999, 3087–3093.
9 D. Gudat, A. W. Holderberg, N. Korber, M. Nieger and M. Schrott, *Z. Naturforsch., B: Chem. Sci.*, 1999, **54**, 1244–1252.
10 T. S. Lobana, P. Kaur and T. Nishioka, *Inorg. Chem.*, 2004, **43**, 3766–3767.
11 G. A. Bowmaker, G. R. Clark and D. K. P. Yuen, *J. Chem. Soc., Dalton Trans.*, 1976, 2329–2334.
12 J. A. Rusanova, K. V. Domasevitch, O. Y. Vassilyeva, V. N. Kokozay, E. B. Rusanov, S. G. Nedelko, O. V. Chukova, B. Ahrens and P. R. Raithby, *J. Chem. Soc., Dalton Trans.*, 2000, 2175–2182.
13 N. P. Rath and E. M. Holt, *J. Chem. Soc., Chem. Commun.*, 1985, 665–667.
14 H. Hartl, I. Brudgam and F. Mahdjourhassanabadi, *Z. Naturforsch., B: Chem. Sci.*, 1985, **40**, 1032–1039.
15 A. Pfitzner and D. Schmitz, *Z. Anorg. Allg. Chem.*, 1997, **623**, 1555–1560.
16 Oxford Diffraction Ltd, Yanton, England, 2008.
17 G. Oszlanyi and A. Süto, *Acta Crystallogr., Sect. A: Found. Crystallogr.*, 2004, **60**, 134–141.
18 L. Palatinus and G. Chapuis, *J. Appl. Crystallogr.*, 2007, **40**, 786–790.
19 V. Petricek, M. Dusek and L. Palatinus, *Jana2000, The crystallographic computing system*, Institute of Physics, Praha, Czech Republic, 2000.
20 A. D. Becke, *J. Chem. Phys.*, 1993, **98**, 5648–5652.
21 M. J. Frisch, G. W. Trucks, H. B. Schlegel, G. E. Scuseria, M. A. Robb, J. R. Cheeseman, G. Scalmani, V. Barone, B. Mennucci, G. A. Petersson, H. Nakatsuji, M. Caricato, X. Li, H. P. Hratchian, A. F. Izmaylov, J. Bloino, G. Zheng, J. L. Sonnenberg, M. Hada, M. Ehara, K. Toyota, R. Fukuda, J. Hasegawa, M. Ishida, T. Nakajima, Y. Honda, O. Kitao, H. Nakai, T. Vreven, J. A. Montgomery, Jr, J. E. Peralta, F. Ogliaro, M. Bearpark, J. J. Heyd, E. Brothers, K. N. Kudin, V. N. Staroverov, R. Kobayashi, J. Normand, K. Raghavachari, A. Rendell, J. C. Burant, S. S. Iyengar, J. Tomasi, M. Cossi, N. Rega, N. J. Millam, M. Klene, J. E. Knox, J. B. Cross, V. Bakken, C. Adamo, J. Jaramillo, R. Gomperts, R. E. Stratmann, O. Yazyev, A. J. Austin, R. Cammi, C. Pomelli, J. W. Ochterski, R. L. Martin, K. Morokuma, V. G. Zakrzewski, G. A. Voth, P. Salvador, J. J. Dannenberg, S. Dapprich, A. D. Daniels, Ö. Farkas, J. B. Foresman, J. V. Ortiz, J. Cioslowski, D. J. Fox, Gaussian, Inc., Wallingford, CT, 2009.
22 D. Figgen, G. Rauhut, M. Dolg and H. Stoll, *Chem. Phys.*, 2005, **311**, 227–244.
23 K. A. Peterson and C. Puzzarini, *Theor. Chem. Acc.*, 2005, **114**, 283–296.
24 K. A. Peterson, B. C. Shepler, D. Figgen and H. Stoll, *J. Phys. Chem. A*, 2006, **110**, 13877–13883.
25 M. Cossi, G. Scalmani, N. Rega and V. Barone, *J. Chem. Phys.*, 2002, **117**, 43–54.
26 M. Vitale, W. E. Palke and P. C. Ford, *J. Phys. Chem.*, 1992, **96**, 8329–8336.
27 M. Vitale, C. K. Rye, W. E. Palke and P. C. Ford, *Inorg. Chem.*, 1994, **33**, 561–566.
28 F. De Angelis, S. Fantacci, A. Sgamellotti, E. Cariati, R. Ugo and P. C. Ford, *Inorg. Chem.*, 2006, **45**, 10576–10584.